Rapid regulated dense-core vesicle exocytosis requires the CAPS protein

M. Rupnik*†, M. Kreft*†, S. K. Sikdar*‡, S. Grilc*, R. Romih§, G. Zupančič*, T. F. J. Martin¶, and R. Zorec*‖

*Laboratory of Neuroendocrinology-Molecular Cell Physiology, Institutes of Pathophysiology and §Cell Biology, Medical School, Ljubljana, Slovenia SI-1001; and ¶Department of Biochemistry, University of Wisconsin, Madison, WI 53706

Edited by Bertil Hille, University of Washington, Seattle, WA, and approved March 1, 2000 (received for review August 23, 1999)

Although many proteins essential for regulated neurotransmitter and peptide hormone secretion have been identified, little is understood about their precise roles at specific stages of the multistep pathway of exocytosis. To study the function of CAPS (Ca^{2+}-dependent activator protein for secretion), a protein required for Ca^{2+}-dependent exocytosis of dense-core vesicles, secretory responses in single rat melanotrophs were monitored by patch-clamp membrane capacitance measurements. Flash photolysis of caged Ca^{2+} elicited biphasic capacitance increases consisting of rapid and slow components with distinct Ca^{2+} dependencies. A threshold of $\approx$10 μM Ca^{2+} was required to trigger the slow component, while the rapid capacitance increase was recorded already at a intracellular Ca^{2+} activity < 10 μM. Both kinetic membrane capacitance components were abolished by botulinum neurotoxin B or E treatment, suggesting involvement of SNARE (soluble *N*-ethylmaleimide-sensitive factor attachment protein receptor)-dependent vesicle fusion. The rapid but not the slow component was inhibited by CAPS antibody. These results were further clarified by immunocytochemical studies that revealed that CAPS was present on only a subset of dense-core vesicles. Overall, the results indicate that dense-core vesicle exocytosis in melanotrophs occurs by two parallel pathways. The faster pathway exhibits high sensitivity to Ca^{2+} and requires the presence of CAPS, which appears to act at a late stage in the secretory pathway.

capacitance | pituitary cells | rat melanotrophs

The application of caged-Ca^{2+} compounds to study Ca^{2+}-dependent exocytosis by membrane capacitance (C_m) measurements has revealed multiple kinetic components in this important process (1). There are two views about the nature of this kinetic diversity. On one side, a sequence of intermediates of a homogeneous population of vesicles may result in multiple kinetic components (2–4). On the other hand, heterogeneous populations of vesicles engaged in distinct pathways of exocytosis also may result in multiple kinetic components. While the quantitative C_m measurements cannot readily distinguish the contributions of heterogeneous vesicles or vesicle intermediates, a combination with other approaches was used to address this problem. Using serotonin-loaded dense-core vesicles and amperometry, it was shown that in pancreatic β cells two populations of dense-core granules enter distinct pathways of exocytosis (5). Using myoballs to monitor the release of acetylcholine from PC12 cells, it was elegantly demonstrated that exocytosis of synaptic vesicles and dense-core granules consists of distinct pathways (6).

An ideal approach to distinguish between the exocytic pathways of synaptic and dense-core vesicles studied by C_m measurements would be a strategy that targets a molecule specifically associated with the release from only one type of secretory organelle. A candidate for such a protein is CAPS (Ca^{2+}-dependent activator protein for secretion), a neural/endocrine-specific 145-kDa protein, originally characterized as a brain cytosolic factor that reconstitutes Ca^{2+}-dependent secretion in permeable neuroendocrine cells (7). CAPS is present on dense-core but not synaptic vesicles in brain homogenates (8). Consistent with a distinct role in dense-core vesicle exocytosis, CAPS was found to be essential for Ca^{2+}-dependent norepinephrine but not glutamate secretion in functional studies with permeable brain synaptosomes (9). In addition, the phenotype of loss-of-function mutants in *Caenorhabditis elegans* CAPS (UNC-31 protein) is distinct from that of mutants in other synaptic proteins such as synaptobrevin (10, 11). The unc-31 phenotype has been attributed in part to a deficit in the secretion of transmitters stored in dense-core vesicles such as the biogenic amines (12).

Using rat melanotrophs, which secrete proopiomelanocortin-derived peptides via dense-core vesicle exocytosis (13), we have used C_m measurements (14) combined with flash photolysis to deliver rapid and spatially homogeneous steps in cytosolic Ca^{2+} (15), which elicit multiple kinetic components in secretory activity of melanotrophs (3, 16). We report that a neutralizing CAPS antibody inhibits the rapid but not the slow component of the Ca^{2+}-dependent capacitance increase, implying that CAPS is required for a late step in exocytosis. Moreover the data reveal an unanticipated functional heterogeneity among dense-core vesicles with respect to Ca^{2+} sensitivity and latency to exocytosis. This heterogeneity was attributed to a distinct role for CAPS on a subset of dense-core vesicles that undergo rapid exocytosis with a high sensitivity to Ca^{2+}.

Materials and Methods

Cell Preparation and Immunocytochemistry. Melanotrophs were prepared as described (17). For immunocytochemistry cells were washed with PBS, fixed for 15 min in 4% paraformaldehyde in PBS, then incubated (10 min) in fixative (0.1% of Triton X-100), and washed with PBS. Nonspecific staining was reduced by incubating cells in 3% BSA and 10% normal goat serum in PBS. Cells then were incubated with primary antibodies (rabbit anti-CAPS antibodies FP5 (9, 36) diluted 1:100, rabbit anti-α-melanocyte-stimulating hormone (MSH) (Peninsula Laboratories) diluted 1:200 and mouse antisynaptotagmin I (18, 19) diluted 1:2,000 in PBS containing 3% BSA) for 2 h at 37°C, washed and incubated in PBS containing CY3-labeled anti-rabbit secondary antibodies (1:200) or FITC anti-mouse secondary antibodies (1:200) and 3% BSA for 45 min. A Light Antifade Kit (Molecular Probes) was used for mounting. Cells were monitored with a confocal microscope (Zeiss, LSM 510,

This paper was submitted directly (Track II) to the PNAS office.

Abbreviations: CAPS, Ca^{2+}-dependent activator protein for secretion; SNARE, soluble *N*-ethylmaleimide-sensitive factor attachment protein receptor; MSH, melanocyte-stimulating hormone; C_m, membrane capacitance; $[Ca^{2+}]$, Ca^{2+} concentration; $[Ca^{2+}]_i$, intracellular Ca^{2+} concentration.

†M.R. and M.K. contributed equally to this work.

‡Present address: Molecular Biophysics Unit, Indian Institute of Science, Bangalore, India.

‖To whom reprint requests should be addressed. E-mail: robert.zorec@pafi.mf.uni-lj.si.

The publication costs of this article were defrayed in part by page charge payment. This article must therefore be hereby marked "*advertisement*" in accordance with 18 U.S.C. §1734 solely to indicate this fact.

Article published online before print: *Proc. Natl. Acad. Sci. USA*, 10.1073/pnas.090359097. Article and publication date are at www.pnas.org/cgi/doi/10.1073/pnas.090359097

objective ×63, numerical aperture = 1.4). CY3 and FITC was excited with a He/Ne (543 nm) or argon (488 nm) laser. Emission signal was filtered by using a LP 595 nm or a narrow band (505–530 nm) filter. Emission images were analyzed by creating an array (mask) of colocalized pixels, the intensities of which were >33% of the maximal image intensity (20). For electron microscopy of CAPS immunogold labeling, pituitary pars intermedia was removed and placed in fixative (2% paraformaldehyde and 0.05% glutaraldehyde in 0.1 M phosphate buffer, pH 7.4), incubated for 1 h at room temperature, and rinsed in the same buffer. Dehydration was performed as follows: 30% ethanol for 30 min at 0°C, 50% ethanol for 30 min (−20°C), 70% ethanol for 30 min (−35°C), and 100% ethanol for 60 min (−35°C). Dehydrated material was infiltrated in 100% ethanol/Lowicryl K4 M (2:1) for 60 min; 100% ethanol/Lowicryl K4 M (1:1) for 60 min; 100% ethanol/Lowicryl K4 M (1:2); 100% Lowicryl K4 M for 60 min, and 100% Lowicryl K4 M overnight; all at −35°C. Polymerization was carried out under UV light for 48 h (−35°C). Ultrathin sections (60–70 nm) were mounted on nickel grids. Nonspecific labeling was blocked by immersing the grids in blocking buffer (0.8% BSA + 0.1% fish gelatin + 5% mouse serum in PBS, pH 7.4) for 30 min. Rabbit anti-CAPS primary antibodies diluted 1:200 in blocking buffer were applied for 18 h (4°C). After rinsing with washing buffer (blocking buffer without mouse serum), the primary antibodies were detected by goat anti-rabbit IgG conjugated to 5 nm gold, diluted 1:50 in blocking buffer for 90 min at room temperature. The grids were rinsed in washing buffer followed by ultrapure water before silver enhancement (4 min) with IntenSE (Amersham Pharmacia). The grids were thoroughly washed in ultrapure water and stained with uranyl acetate and lead citrate. The sections were examined with a Philips CM 100 electron microscope. Control sections were incubated either in the absence of primary antibody, or with an inappropriate first antibody.

Compensated membrane capacitance measurements (14, 21, 22) using a SWAM Cell or SWAM IIB patch-clamp-lock-in amplifier (Celica, Ljubljana, Slovenia), operating at 1.6-kHz lock-in frequency were used. Upon establishment of the whole-cell configuration C_m and G_a (access conductance) were compensated by C_{slow} and G_a compensation controls. Sine voltage of 11–111 mV_{rms} was applied. The phase angle setting was determined by a 100-fF or 1-pF pulse and monitoring the projection of the pulse from the C (signal proportional to C_m) to G outputs of the lock-in amplifier. These two signals were stored unfiltered (C-DAT4, Cygnus Technology, Delaware, PA) for off-line analysis. Simultaneously we recorded filtered (300 Hz, 4 pole Bessel) C and G signals, the fluorescence intensity from a C660 photon counter (Thorn EMI, Ruislip, Middlesex, U.K.) and membrane current (0–10 Hz, low pass). The PHOCAL program (LSR, Cambridge, U.K.) was used to acquire signals every 5 ms. For high temporal resolution measurements of C_m, the records on DAT were played back and a 10-s epoch of the signal enveloping each flash was digitized at 50 kHz by using a CDR program (J. Dempster, University of Glasgow, Strachclyde, U.K.). Signals were digitally filtered at 1 kHz (two-way 150th- order FIR1 filter, Math Works MATLAB) and resampled at 10 kHz. The pipette solution contained 100 mM KCl, 10 mM TEACl 10, 40 mM KOH/Hepes, 2 mM Na_2ATP, 2 mM $MgCl_2$, 4 mM K_4-NP-EGTA [*o*-nitrophenyl ethyleneglycol-bis-(β-aminoethyl-ether)-*N*,*N*,*N*′,N′-tetrapotassium salt], 3.6 mM $CaCl_2$, 0.5 mM furaptra, pH 7.2. The bath contained 131.8 mM NaCl, 5 mM KCl, 2 mM $MgCl_2$, 0.5 mM NaH_2PO_4, 5 mM $NaHCO_3$, 10 mM Na Hepes, 10 mM D-glucose, 1.8 mM $CaCl_2$, pH 7.2. Total EGTA concentration was 4 mM, which exceeds the buffering capacity of melanotrophs (23). Recordings were made at room temperature. Pipette resistances ranged from 1 to 4 MΩ.

Flash Photolysis and Intracellular Ca^{2+} Concentration ($[Ca^{2+}]_i$) Measurements. We used NP-EGTA (Molecular Probes) to manipulate $[Ca^{2+}]_i$. A UV flash from a Xe arc flash lamp (Hi-Tech, Salisbury, U.K.) was delivered to cells through a 40× fluor oil immersion objective of a Nikon Diaphot microscope. The same optical pathway as in flash photolysis was used to illuminate the fluorescent $[Ca^{2+}]$ indicator furaptra (Molecular Probes). Calibration of $[Ca^{2+}]_i$ measurements was performed in each cell (24, 25) by using the autofluorescence in a cell-attached configuration and the fluorescence in a resting whole-cell recording.

Microinjection. Transjector 4657 with a micromanipulator (Eppendorf, Germany) was used. Pulses (8–12 hPa, 0.3–1 s) were applied with a compensation pressure (1 hPa). Microinjection solution consisted of 150 mM K-gluconate, 2 mM $MgCl_2$, 10 mM Hepes, 6 mg/ml rhodamine isothiocyanate, 2–20 mg/ml antibody. Pipettes were prepared with a horizontal puller (P-87, Sutter Instruments, Novato, CA). Microinjected cells were identified with coinjection of rhodamine-labeled dextran (Sigma, 25 kDa). Injection of dextran marker alone did not affect secretory responses *per se*. Botulinum neurotoxin B (a gift from Das Gupta, University of Wisconsin, Madison and Dušan Šuput, Medical Faculty, Ljubljana, Slovenia) or botulinum neurotoxin E light chain was microinjected into cells (20 ng/μl) together with the dextran marker. Before continuing with patch-clamp experiments the cells were allowed to rest for 1–2 h at 37°C.

Results

Subcellular Localization of CAPS in Rat Melanotrophs. As anticipated from previous studies on the selective expression of CAPS in neural and endocrine tissues (7, 10), CAPS was found to be expressed in rat melanotrophs (Fig. 1*A*). A punctate pattern of immunofluoresence was detected throughout the cytoplasm and cell periphery of melanotrophs in confocal microscopy (Fig. 1*B*). Melanotrophs contain numerous dense-core vesicles that store adrenocorticotropic hormone or α-MSH and β-endorphin (13, 26). Localization of CAPS to some of the dense-core vesicles was revealed by immunogold electron microscopy using purified CAPS antibody (Fig. 1*C*). To test further whether CAPS localizes to dense-core vesicles, double immunofluorescent studies with antibodies to a vesicle membrane protein (synaptotagmin I), vesicle cargo (α-MSH), and CAPS were conducted.

The cytofluorograms shown in Fig. 2*A* represent the pixels measured in the synaptotagmin I (*Left*) and α-MSH (*Center*) images and the mask (*Right*) was constructed from the colocalized pixels. This result confirmed that synaptotagmin I is entirely present on the secretory vesicles in rat melanotrophs. In contrast, a similar experiment (Fig. 2*B*) where anti-CAPS antibody was used instead of the anti-α-MSH antibody revealed that CAPS corresponded to a subset of the dense-core vesicles labeled by synaptotagmin I antibodies (Fig. 2*B Right*).

Flash-Induced Rapid and Slow C_m Increases Differ in Ca^{2+} Sensitivity. Previously, dimethoxy-nitrophen (DMN), a Ca^{2+}-cage compound was used to study the Ca^{2+} dependence of C_m increase in rat melanotrophs (3). DMN has a poor selectivity in binding Ca^{2+} over Mg^{2+}. Therefore, we used NP-EGTA that permits large and rapid changes in $[Ca^{2+}]_i$ to be elicited in the presence of physiological $[Mg^{2+}]_i$ (27). Parsons *et al.* (28) used NP-EGTA in rat melanotrophs, but a detailed study of Ca^{2+} dependence of C_m increase was not performed.

A UV light flash that photolyzed ≈20% of the loaded Ca^{2+}-bound NP-EGTA activated a biphasic C_m response in melanotrophs (Fig. 3 *A* and *B*) similar to responses observed previously in other cells (2–6, 15, 16, 29). The flash discharge transiently elevated Ca^{2+} to 25 μM, which returned to baseline exponentially with a time constant of 3.6 s (Fig. 3*A Lower*). Increased Ca^{2+} elicited a large rise in C_m by 1,125 fF within 10 s

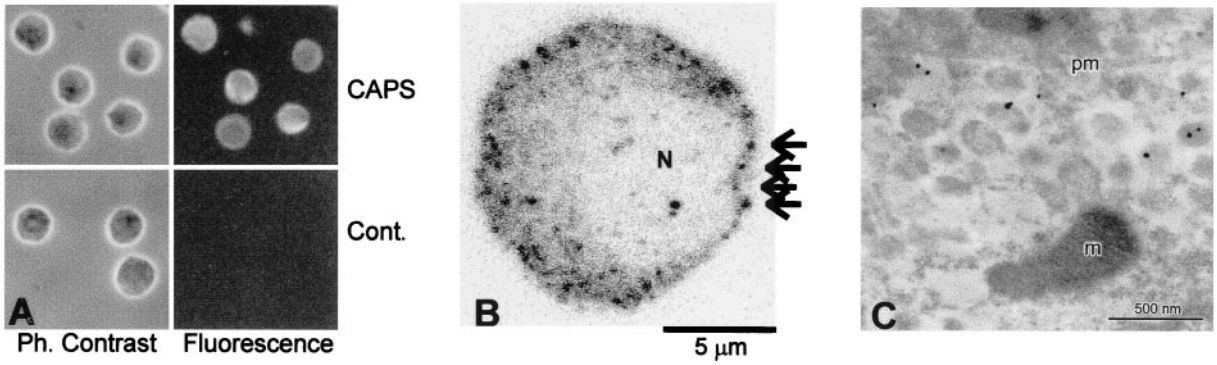

Fig. 1. Subcellular localization of CAPS in rat melanotrophs. (*A*) Immunocytochemical detection of CAPS in rat melanotrophs. (*Upper*) Phase contrast and corresponding immunofluoresence image of CAPS labeled cells. (*Lower*) Phase contrast and the corresponding immunofluorescence image of cells stained with the preimmune serum. (*B*) Confocal immunocytochemical detection of CAPS in rat melanotrophs. Note that fluorescence intensity was inversed, such that white denotes background and black a signal from fluorophore: N, nucleus, arrows point to punctate appearance of stain. (*C*) Electron micrograph of a rat melanotroph showing secretory vesicles near the plasmamembrane (pm), labeled by immunogold particles indicating the presence of CAPS on secretory vesicles. m, mitochondrion. (Scale bar = 500 nm).

after which a decrease caused by endocytosis was observed (Fig. 3*A Upper*). At higher time resolution, a smaller (120 fF) transient rise in C_m was observed within the first 100 ms after the flash (Fig. 3*B Upper*). The initial transient rise and subsequent larger C_m increase were termed the rapid and slow components, respectively. The rapid rise in C_m was followed by a decline determined by endocytosis. In 19 of 75 cells, C_m declined below resting C_m because of excess retrieval (30). When the NP-EGTA in the pipette lacked Ca^{2+}, a UV flash failed to elevate Ca^{2+} and neither rapid nor slow exocytosis were observed (not shown). The amplitude B for the rapid component was measured as the positive peak value in C_m (relative to the C_m value preceding the flash) during the first 100 ms after the flash, whereas the amplitude A of the slow exocytosis was determined as the positive peak value in C_m after the time point of 100 ms (Fig. 3).

The amplitudes and rates of the rapid and slow components of the C_m increase depended on the Ca^{2+} levels achieved during uncaging of the Ca^{2+}-NP-EGTA (Fig. 4, open symbols). The amplitude of the rapid phase (167 ± 11 fF, mean ± SEM, n = 75) exhibited a threshold at very low Ca^{2+} and was maximal by 5 μM (Fig. 4*Ac*), indicating a very high affinity Ca^{2+}-dependent process. In contrast, the amplitude of the slow phase increased with Ca^{2+} beyond a threshold of ≈10 μM, indicating a much lower affinity Ca^{2+}-dependent process (Fig. 4*Ab*). Time derivatives of C_m traces confirmed the observation that flash-induced increases in C_m consist of rapid and slow components (Fig. 4*Ba*). The maximal rate of C_m increase (1,916 ± 133 fF/s, n = 75) of the rapid component was maximal by 5 μM Ca^{2+} (Fig. 4*Bc*), whereas the rate of maximal increase of the slower component increased beyond a threshold of ≈10 μM Ca^{2+} (Fig. 4*B a* and *b*).

Rapid Component of C_m Increase Is Blocked by CAPS Antibody. Injection of CAPS antibody strongly affected the flash-evoked biphasic C_m increase. Of 17 injected cells 16 exhibited C_m responses that were devoid of the rapid component (Fig. 5*A*).

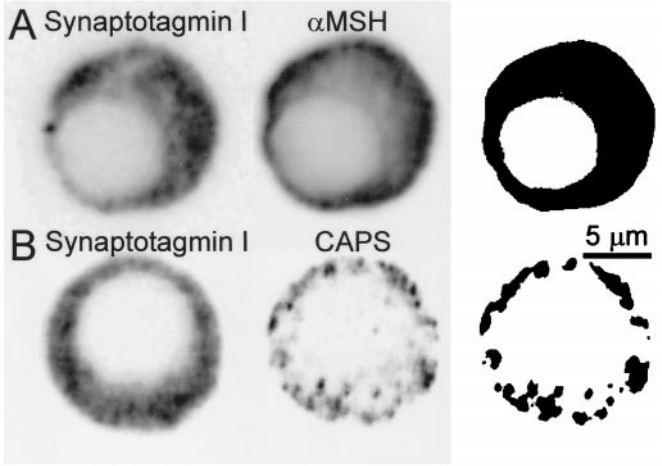

Fig. 2. Subcellular distribution of synaptotagmin I, α-MSH, and CAPS in rat melanotrophs. Double immunofluorescence confocal micrographs obtained with mouse antisynaptotagmin I antibodies (*Left*) and rabbit anti-α-MSH antibodies (*A, Center*) or anti-CAPS antibodies (*B, Center*). Immunoreactivity was detected with CY3-conjugated anti-rabbit and fluorescein-conjugated anti-mouse antibodies. Optical sections were taken through the center of the nucleus. Cell diameter is around 12 μm. (*Right*) The images show the masks obtained after selection of the pixels double-labeled with CY3 and fluorescein from the two-dimensional scatter histograms of gray values. The colocalization of two images in *B* (*Right*) indicates that synaptotagmin I and CAPS are colocalized to a subset of vesicles. Fluorescence intensity was inversed as in Fig. 1.

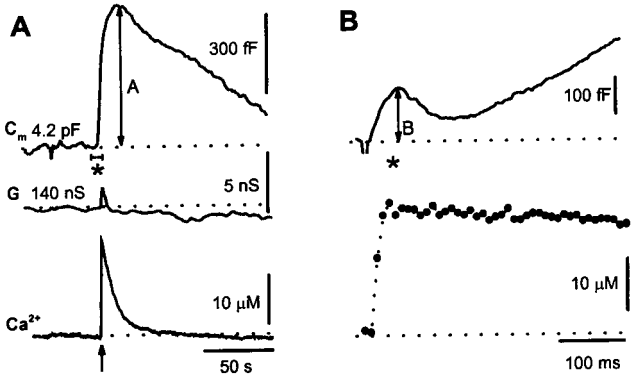

Fig. 3. (*A*) Time-dependent changes in flash-induced changes in C_m at low time resolution. A flash application (arrow) elicited a transient in $[Ca^{2+}]_i$ (*Bottom*). Dashed line represents resting C_m of 4.2 pF [resting C_m was 5.3 ± 0.2 pF (mean ± SEM, n = 50)]. The maximum amplitude of the Ca^{2+}-induced rise in C_m (slow exocytosis) is indicated by A. G shows conductance, which reflects changes in access conductance, membrane conductance, and C_m. Access conductance (140 nS, dashed line) was determined with controls on the SWAM amplifier. (*B*) Expanded high time resolution of C_m trace from *A*, labeled by *. Changes in C_m after a flash (arrow)-induced increase in $[Ca^{2+}]_i$ (*Lower*) and C_m (*Upper*). B indicates the amplitude of the early rapid C_m response.

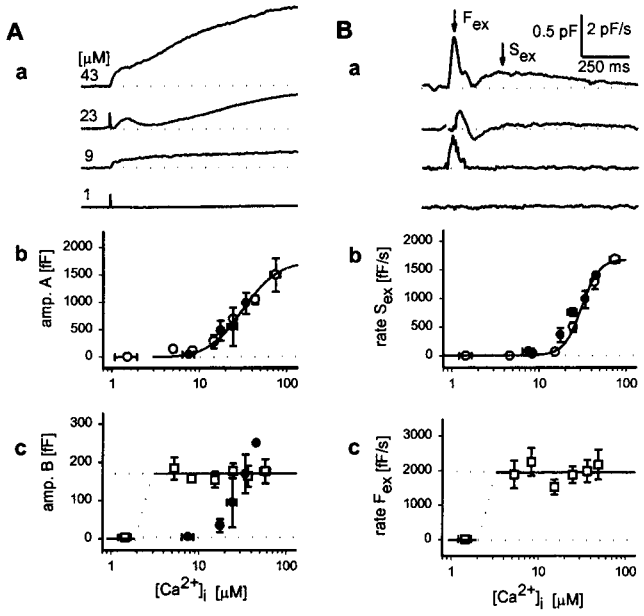

Fig. 4. Ca^{2+} dependence of rapid and slow kinetic components of C_m. (*A*) (*a*) Four examples of flash-induced C_m traces recorded at different peak $[Ca^{2+}]_i$ (indicated at the beginning of each trace). Artefacts denote flash delivery. Relationship between the peak $[Ca^{2+}]_i$ and the amplitude of slow component (*b*) is depicted by ○, whereas the amplitude of the rapid component of exocytosis (*c*) is shown by □. Each point represents 3–25 averaged measurements. Error bars indicate SEM. Curve fitted through points in *b* is of the form: $C_m = (1{,}753[Ca^{2+}]^2)/(K_d^2 + [Ca^{2+}]^2)$, where C_m is in fF and K_d (30.2 μM) represents the $[Ca^{2+}]$ at which the response in C_m is half-maximal. Amplitude *B* was not correlated to $[Ca^{2+}]_i$, the line represents the mean amplitude of the rapid exocytosis (167 fF). Filled symbols show the effect of CAPS antibody injection on measured parameters. (*B*) (*a*) Time derivatives of traces shown in *Aa*. Two maxima are indicated by arrows (F_{ex} and S_{ex} denoting rapid and slow exocytosis). Relationship between peak $[Ca^{2+}]_i$ and S_{ex} is shown in *b* (○) and F_{ex} in *c* (□). Each point represents 4–28 averaged measurements. Error bars indicate SEM. The curve drawn through points in *b* represents a best fit obtained by the SIGMAPLOT nonlinear regression algorithm and is of the form: $dC_m/dt = (A[Ca^{2+}]^n)/(K_d^n + [Ca^{2+}]^n)$, where A = 1,678 ± 125 fF/s, n = 4.3 ± 0.7; K_d = 30.7 ± 1.7 μM; all parameters are in the format mean ± SEM, $P <$ 0.0001. Data points larger than 5 μM $[Ca^{2+}]$ in *c* showed no apparent dependence of dC_m/dt and $[Ca^{2+}]$, the line drawn equals the average value of 1,916 fF/s. Filled symbols show the effect of CAPS antibody injection on maximal dC_m/dt, *b*). Note that in these experiments responses are characterized by only one maximum in dC_m/dt (see Fig. 5*A*).

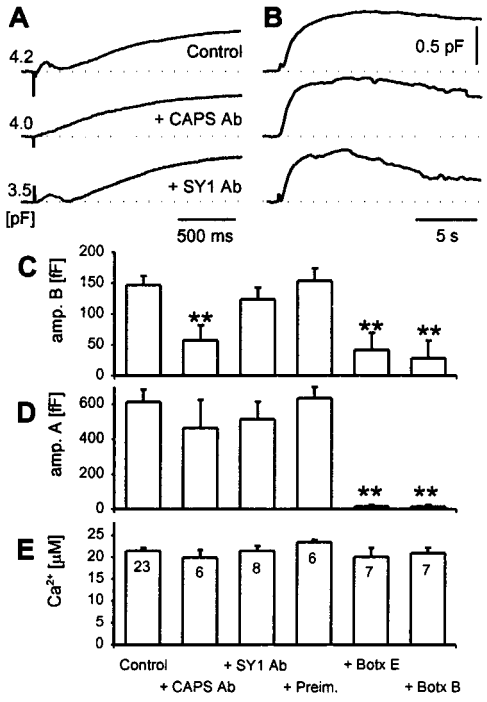

Fig. 5. Rapid component of C_m increase is blocked by CAPS antibody. Three examples of time-dependent changes in C_m induced by caged photolysis of NP-EGTA (artefacts) in a control cell, in a cell preinjected with anti-CAPS serum (+CAPS Ab), and in a cell preinjected by an antisynaptotagmin I/II antibody (31) (SY1 Ab). Responses in C_m to 21, 21, and 20 μM peak $[Ca^{2+}]$ transients (control, CAPS Ab, and SY1 Ab, respectively) are shown at high (*A*) and slow (*B*) time resolution. *A* shows early responses where the amplitudes for rapid exocytosis is easily noticed in control and SY1 Ab-treated cells, whereas in *B* 25s epochs are shown to highlight the slow exocytosis. (*C*) Mean amplitude of the rapid kinetic component (amp. B) and (*D*) mean amplitude of the slow kinetic component (amp. A) of the biphasic secretory response elicited by a transient increase in $[Ca^{2+}]_i$ by UV flash photolysis in control cells, cells preinjected with CAPS Ab (+CAPS Ab), SY1 Ab (+SY1 Ab), protein A-Sepharose purified Ig fractions from sera of nonimmunized animals (+Preim.), and botulinum neurotoxins B (+Botx B) and E (+Botx E). (*E*) Average peak response in $[Ca^{2+}]_i$ elicited by UV flash photolysis of Ca^{2+}-loaded NP-EGTA. Numbers adjacent to columns in *E* indicate numbers of cells studied. Error bars indicate SEM, and * indicate significant differences compared with the control (**, $P < 0.01$, Student's *t* test).

With IgGs from immune CAPS serum, only monotonic increases in C_m were observed (Fig. 5*A Middle*), whereas cells injected with IgGs from preimmune serum exhibited biphasic C_m increases indistinguishable from those of uninjected cells (compare Fig. 4*A* with Fig. 5*A Top*). The amplitude and the Ca^{2+} sensitivity of responses observed after CAPS antibody injection was similar to that of slow exocytosis in nonimmune antibody-injected or uninjected cells (Fig. 4, filled symbols; Fig. 5), whereas the amplitude of the rapid component was strongly inhibited and exhibited a decreased Ca^{2+} sensitivity (Fig. 4*Ac*, filled symbols).

Interestingly, injection of an antisynaptotagmin I/II C2A domain antibody that was previously shown to block secretion from chromaffin cells (31) did not affect the time course of C_m changes in melanotrophs (Fig. 5). The results indicate a specificity for the CAPS antibody inhibition because another antibody that binds to dense-core vesicles in melanotrophs failed to affect rapid exocytosis.

Rapid and Slow Components of Capacitance Increase Are Blocked by Botulinum Toxins B and E. The SNARE (soluble *N*-ethylmaleimide-sensitive factor attachment protein receptor) proteins synaptobrevin/VAMP (vesicle-associated membrane protein), syntaxin, and SNAP-25 are essential constituents for exocytosis in neuroendocrine cells (32, 33) and constitute molecular targets for the clostridial neurotoxin proteases (34). To determine whether the rapid and slow C_m increases observed in melanotrophs were mediated by SNARE protein-dependent processes, botulinum neurotoxins were injected into the cells before patch-clamp determinations. Injection of botulinum neurotoxin B, which proteolytically cleaves synaptobrevin/VAMP, completely abolished the slow component of C_m (Fig. 6) and strongly inhibited the rapid component of exocytosis. Similar results were obtained with the injection of botulinum neurotoxin E (Fig. 5), which proteolytically cleaves SNAP-25. The results indicate that both rapid and slow phases of the Ca^{2+}-dependent exocytosis in melanotrophs are SNARE protein-dependent processes and are caused by vesicular fusion.

Discussion

CAPS initially was characterized as a cytosolic factor required for Ca^{2+}-activated dense-core vesicle exocytosis in permeabilized neuroendocrine cells (7, 10). Two recent studies indicate

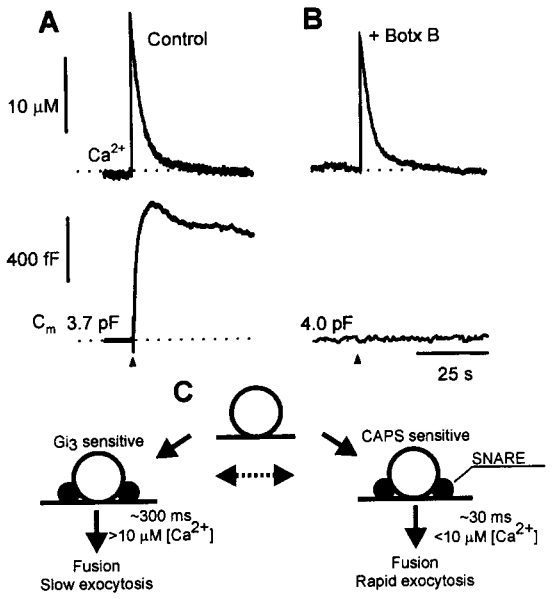

Fig. 6. Botulinum toxin B pretreatment inhibits changes in C_m. Time-dependent changes in $[Ca^{2+}]_i$ (*Upper*) and C_m (*Lower*) in (*A*) a control cell and (*B*) in a cell pretreated by botulinum neurotoxin B (+ Botx B). Note the complete absence in a rise in C_m after the flash-induced rise in $[Ca^{2+}]_i$ (*Upper*). Dotted lines indicate resting $[Ca^{2+}]_i$ and C_m. (*C*) Model describing CAPS- and $G\alpha_{i3}$-antibody action (25) on kinetic components of C_m. Vesicles entering rapid and slow exocytosis are recruited from a common pool that appears to be closely associated with the plasmamembrane (25). From this pool vesicles exocytose along biochemically distinct mechanisms. Typical reaction time constants and threshold $[Ca^{2+}]_i$ for the CAPS-antibody- and $G\alpha_{i3}$-antibody-sensitive pathways are indicated near the arrows. Endocytosis is not depicted but is assumed to proceed for each type of exocytosis separately. The possibility that the two functional states of exocytosis can be interconverted is indicated by the broken arrow.

that CAPS may be an essential constituent that selectively functions in the dense-core vesicle but not synaptic vesicle exocytotic pathway. First, CAPS is present on dense-core but not synaptic vesicles in brain homogenates (8). Second, in functional assays with permeable brain synaptosomes, neutralizing CAPS antibodies interfere with Ca^{2+}-triggered norepinephrine but not glutamate release (9). Consistent with a role in dense-core vesicle exocytosis, the present immunocytochemical studies localized CAPS to dense-core vesicles in melanotrophs (Fig. 1*C*). These, however, appeared to represent a subset of the entire population of vesicles that were labeled with synaptotagmin I (Fig. 2*B*). These studies indicate that, whereas all vesicles appeared to contain synaptotagmin I, only a subset were endowed with CAPS.

Studies of regulated dense-core vesicle exocytosis in permeable PC12 cells or membrane fractions from these cells (7, 10, 35, 36) revealed that CAPS is essential for a late Ca^{2+}-triggered step beyond vesicle docking and priming. To determine the stage at which CAPS is required for exocytosis in melanotrophs, we stimulated exocytosis by flash photolysis of caged Ca^{2+} (15) while monitoring C_m increases (14). Previous experiments using similar approaches in a variety of neuroendocrine cells reported complex kinetic responses consisting of at least two components (2–6, 15, 16, 29). Similarly, in the present studies in melanotrophs, a step rise in $[Ca^{2+}]$ elicited two primary kinetic phases of C_m increase (Fig. 3), a rapid ($t_{1/2} \approx 50$ ms) and a slow ($t_{1/2} \approx 500$ ms) component. However, our results differ from those reported (3) where the rapid and the slow components exhibited a similar Ca^{2+} sensitivity, with a threshold at ≈ 10 μM $[Ca^{2+}]_i$. In our study the rapid component was maximally activated by 5 μM $[Ca^{2+}]_i$ (Fig. 4), whereas the slow component exhibited a similar Ca^{2+} sensitivity to that reported (3).

Injection of CAPS antibodies was found to completely inhibit the rapid C_m increase, which provides direct evidence that CAPS is essential for a late step in the dense-core vesicle exocytotic pathway. Surprisingly, however, CAPS antibody inhibition was highly selective in inhibiting the rapid but not the slow component of the C_m increase (Fig. 5).

Multiple kinetic components of C_m increase previously have been interpreted to reflect different states of vesicles along a sequential exocytotic pathway (3, 4, 15). However, the biphasic C_m increase observed in the present studies is more likely to be caused by the operation of two distinct Ca^{2+}-dependent pathways (see ref. 1). Otherwise, it is difficult to explain how complete antibody inhibition of the fast C_m component is followed by an unimpeded subsequent slow C_m component because inhibition of both components would be expected if they shared a common antibody-sensitive step. Both components do appear to use common SNARE protein-dependent steps as indicated by their similar susceptibility to inhibition by clostridial neurotoxins (Fig. 6*B*). The rapid component was less sensitive to the botulinum neurotoxin treatment (Fig. 5), which may indicate that vesicles entering the slow exocytosis are characterized by a loose form of the SNARE complex and those that undergo rapid exocytosis by a tight form of the SNARE complex (37). Xu *et al.* (37) interpreted that the two pools of vesicles that share a similar Ca^{2+} sensitivity, are coupled sequentially, although a parallel pathway of exocytosis could not be excluded experimentally. Interestingly, our studies of the Ca^{2+} sensitivity of exocytosis (Fig. 4) reinforce the view that rapid and slow C_m components represent parallel exocytotic pathways that are regulated in a distinct manner (Fig. 6*C*). The rapid pathway strongly inhibited by CAPS antibody also exhibited a distinct high sensitivity to triggering at low $[Ca^{2+}]_i$ (Fig. 4). In contrast, the slow pathway that was CAPS antibody insensitive was only elicited at $[Ca^{2+}]_i$ exceeding 10 μM (Fig. 4). Each pathway also is coupled to distinct endocytic pathways that exhibit characteristic time constants for the C_m decline (not shown).

In PC12 cells, a biphasic increase in C_m was interpreted to result from fusion of synaptic vesicles followed by the fusion of dense-core vesicles vesicles (6, 29). In contrast, several lines of evidence indicate that the two kinetic components of the C_m increase in melanotrophs represent exocytosis of dense-core vesicles (5). First, the rapid increase in C_m that is sensitive to CAPS antibody likely corresponds to a subset of vesicles identified by confocal microscopy (Fig. 2). Second, although the slow component of the C_m rise requires higher $[Ca^{2+}]$ similar to that of synaptic vesicle exocytosis (38), it is usually the case that synaptic vesicle exocytosis occurs more rapidly than that of dense-core vesicles when both pathways are present (29, 39). Third, if the C_m of a synaptic vesicle is 50–100 aF, our data indicate that a population of 10,000-20,000 vesicles are required to account for the slow phase. Such a population of small clear vesicles would be difficult to overlook in electron microscopy. Moreover, synaptophysin, a marker of synaptic vesicles (40), was not detected in rat melanotrophs (41). It is likely that the slow component of the C_m increase is also caused by the fusion of dense-core vesicles. Melanotrophs contain about 3,000 dense-core vesicles that are morphologically docked (42). With an average C_m of 2 fF per vesicle (43), this pool of docked dense-core vesicles can readily account for the rapid and slow components of the C_m increase. CAPS antibody also may act on unidentified synaptic-like vesicles in melanotrophs.

Fusion of a rapid release pool of synaptic vesicles in nerve terminals is triggered by high $[Ca^{2+}]$ operating on a low affinity Ca^{2+} receptor (44). In contrast, the rapid component of the C_m rise in melanotrophs exhibited a very high Ca^{2+} sensitivity whereas the slow component was activated only at high $[Ca^{2+}]$

(Fig. 4). The molecular basis for the varying Ca^{2+} sensitivities of regulated exocytotic pathways remains to be established. Synaptotagmins, a family of C2 domain-containing vesicle proteins that bind phospholipids and SNARE proteins in a Ca^{2+}-dependent manner, are essential for regulated exocytosis (45). High and low Ca^{2+} affinity isoforms of synaptotagmin expressed in neural and endocrine cells have been suggested as potential Ca^{2+} sensors for dense-core vesicle and synaptic vesicle exocytosis, respectively (46). Whether a heterogeneous distribution of high and low Ca^{2+} affinity isoforms of synaptotagmin on dense-core vesicles in melanotrophs can explain the functional heterogeneity observed in our studies remains to be determined.

CAPS is also a Ca^{2+}-binding protein (10) and its presence on a subset of dense-core vesicles (Fig. 2) could confer altered Ca^{2+} sensitivity for exocytosis. Such a mechanism may be of physiological relevance. Melanotrophs fire sodium and calcium action potentials (47). For secretion to be coupled to these depolarizations, the rate of exocytosis should be sufficiently high. It was shown that depolarization lasting between 2 and 40 ms support an increase in C_m in rat melanotrophs (48). Dense-core vesicles that undergo depolarization-induced exocytosis require around 5 μM Ca^{2+} (49). The time constant of increase of the rapid C_m component of around 30–40 ms (Fig. 3) and the Ca^{2+} sensitivity of the rapid exocytosis (Fig. 4) indicate that an action potential should trigger exocytosis of the vesicles in the rapid pathway in melanotrophs. Moreover, depolarization-induced secretion should be inhibited by CAPS antibody. Recent studies with chromaffin cells have shown that CAPS antibody inhibits depolarization-induced secretion detected by patch-clamp capacitance and amperometric detection of catecholamines (50).

In summary, our data suggest that two kinetic components of regulated exocytosis detected by patch-clamp capacitance measurements in melanotrophs represent parallel pathways of dense-core vesicle-mediated secretion. The results indicate that CAPS is a key component of dense-core vesicles that rapidly fuse at low $[Ca^{2+}]_i$.

We thank M. Kordaš for continuous support, S. Chasserot-Golaz for initial confocal microscopy, M. Seagar for synaptotagmin I antibody, M. Fukuda for synaptotagmin C2A domain antibody, and J.A. Kowalchyk and B.W. Porter for CAPS antibody production. This work was supported by a joint U.S.-Slovenian project (95–471, 9501122), National Institutes of Health Grant DK 40428 (to T.F.J.M.), and Ministry of Science and Technology of the Republic of Slovenia Grants J3 6027 and J3 8722 (to R.Z.).

1. Kasai, H. (1999) *Trends Neurosci.* **22,** 88–93.
2. Heinemann, C., Chow, R. H., Neher, E. & Zucker, R. S. (1994) *Biophys. J.* **67,** 2546–2557.
3. Thomas, P., Wong, J. G., Lee, A. K. & Almers, W. (1993) *Neuron* **11,** 93–104.
4. Xu, T., Binz, T., Niemann, H. & Neher, E. (1998) *Nat. Neurosci.* **1,** 192–200.
5. Takahashi, N., Kadowaki, T., Yazaki, Y., Miyashita, Y. & Kasai, H. (1997) *J. Cell Biol.* **138,** 55–64.
6. Ninomiya, Y., Kishimoto, T., Yamazawa, T., Ikeda, H., Miyashita, Y. & Kasai, H. (1997) *EMBO J.* **16,** 929–934.
7. Walent, J., Porter, B. W. & Martin, T. F. J. (1992) *Cell* **70,** 765–775.
8. Berwin, B., Floor, E. & Martin, T. F. J. (1998) *Neuron* **21,** 137–145.
9. Tandon, A., Bannykh, S., Kowalchyk, J. A., Banerjee, A., Martin, T. F. J. & Balch, W. E. (1998) *Neuron* **21,** 147–154.
10. Ann, K., Kowalchyk, J., Loyet, K. M. & Martin, T. F. J. (1997) *J. Biol. Chem.* **272,** 19637–19640.
11. Avery, L., Bargmann, C. I. & Horvitz, H. R. (1993) *Genetics* **134,** 455–464.
12. Desai, C., Garriga, G., McIntire, S. L. & Horvitz, H. R. (1988) *Nature (London)* **336,** 638–646.
13. Mains, R. E. & Eipper, B. A. (1979) *J. Biol. Chem.* **254,** 7885–7894.
14. Neher, E. & Marty, A. (1982) *Proc. Natl. Acad. Sci. USA* **79,** 6712–6716.
15. Neher, E. & Zucker, R. S. (1993) *Neuron* **10,** 21–30.
16. Thomas, P., Wong, J. G. & Almers, W. (1993b) *EMBO J.* **12,** 303–306.
17. Rupnik, M. & Zorec, R. (1992) *FEBS Lett.* **303,** 221–223.
18. Takahashi, M., Arimatsu, Y., Fujita, S., Fujimoto, Y., Kondo, S., Hama, T. & Miyamoto, E. (1991) *Brain Res.* **551,** 279–292.
19. Leveque, C., Hoshino, T., David, P., Shoji-Kasai, Y., Leys, K., Omori, A., Lang, B., el Far, O., Sato, K., Martin-Moutot, N., *et al*. (1992) *Proc. Natl. Acad. Sci. USA* **89,** 3625–3629.
20. Chasserot-Golaz, S., Vitale, N., Sagot, I., Delouche, B., Dirring, S., Pradel, L. A., Henry, J. P., Aunis, D. & Bader, M. F. (1996) *J. Cell. Biol.* **133,** 1217–1236.
21. Zorec, R., Henigman, F., Mason, W. T. & Kordaš, M. (1991) *Methods Neurosci.* **4,** 194–210.
22. Rupnik, M. & Zorec, R. (1995) *Pflügers Arch.* **431,** 76–83.
23. Thomas, P., Surprenant, A. & Almers, W. (1990) *Neuron* **5,** 723–733.
24. Carter,T. D. & Ogden, D. (1994) *Pflügers Arch.* **428,** 476–484.
25. Kreft, M., Gasman, S., Chasserot-Golaz, S., Kuster, V., Rupnik, M., Sikdar, S. K., Bader, M.-F. & Zorec, R. (1999) *J. Cell Sci.* **112,** 4143–4150.
26. Tanaka, S., Nomizu, M. & Kurosumi, K. (1991) *J. Histochem. Cytochem.* **39,** 809–821.
27. Ellis-Davies, G. C. & Kaplan, J. H. (1994) *Proc. Natl. Acad. Sci. USA* **91,** 187–191.
28. Parsons, T. D., Ellis-Davies, G. C. R. & Almers, W. (1996) *Cell Calcium* **19,** 185–192.
29. Kasai, H., Takagi, H., Ninomiya, Y., Kishimoto, T., Ito, K., Yoshida, A., Yoshioka, T. & Miyashita, Y. (1996) *J. Physiol. (London)* **494,** 53–65.
30. Thomas, P., Lee, A. K., Wong, J. G. & Almers, W. (1994) *J. Cell Biol.* **124,** 667–675.
31. Ohara-Imaizumi, M., Fukuda, M., Niinobe, M., Misonou, H., Ikeda, K., Murakami, T., Kawasaki, M., Mikoshiba, K. & Kumakura, K. (1997) *Proc. Natl. Acad. Sci. USA* **94,** 287–291.
32. Martin, T. F. J. (1997) *Trends Cell Biol.* **7,** 271–276.
33. Burgoyne, R. D. & Morgan, A. (1998) *BioEssays* **20,** 328–335.
34. Montecucco, C. & Schiavo, G. (1994) *Mol. Microbiol.* **13,** 1–8.
35. Hay, J. C. & Martin, T. F. J. (1992) *J. Cell Biol.* **119,** 139–151.
36. Martin, T. F. J. & Kowalchyk, J. A. (1997) *J. Biol. Chem.* **272,** 14447–14453.
37. Xu, T., Rammner, B., Margittai, M., Artalejo, A. R., Neher, E. & Jahn, R. (1999) *Cell* **99,** 713–722.
38. Smith, S. & Augustine, G. J. (1989) *Trends Neurosci.* **11,** 458–465.
39. Jan, L. Y. & Jan, Y. N. (1982) *J. Physiol. (London)* **327,** 219–246.
40. Navone, F., Jahn, R., Gioia, G. D., Stukenbrok, H., Greengard, P. & DeCamilli, P. (1996) *J. Cell Biol.* **103,** 2511–2527.
41. Saland, L. C., Apodaca, A., Ramirez, D., Hernandez, V., Gaddy, J. & Thomas, D. (1997) *Brain Res. Bull.* **43,** 561–564.
42. Parsons, T. D., Coorssen, J. R., Horstmann, H. & Almers, W. (1995) *Neuron* **15,** 1085–1096.
43. Zupančič, G., Kocmur, L., Veraniè, P., Grilc, S., Kordaš, M. & Zorec, R. (1994) *J. Physiol. (London)* **480,** 539–552.
44. Zucker, R. S. (1996) *Neuron* **17,** 1049–1055.
45. Geppert, M. & Südhof, T. C. (1998) *Annu. Rev. Neurosci.* **21,** 75–95.
46. Südhof, T. C. & Rizo, J. (1996) *Neuron* **17,** 379–388.
47. Douglas, W. W. & Taraskewich, P. S. (1980) *J. Physiol. (London)* **326,** 201–211.
48. Mansvelder, H. D & Kits, K. S. (1998) *J. Neurosci.* **18,** 81–922.
49. Chow, R. H., Klingauf, J. & Neher, E. (1994) *Proc. Natl. Acad. Sci. USA* **91,** 12765–12769.
50. Elhamdani, A., Martin, T. F. J., Kowalchyk, J. A. & Artalejo, C. R. (1999) *J. Neurosci.* **19,** 7375–7383.